

Valentina Grishko, Viktor Pastukh, Viktoriya Solodushko, Mark Gillespie, Junichi Azuma and Stephen Schaffer

Am J Physiol Heart Circ Physiol 285:2364-2372, 2003. First published Aug 14, 2003;
doi:10.1152/ajpheart.00408.2003

You might find this additional information useful...

This article cites 43 articles, 25 of which you can access free at:

<http://ajpheart.physiology.org/cgi/content/full/285/6/H2364#BIBL>

This article has been cited by 6 other HighWire hosted articles, the first 5 are:

Alpha2-Antiplasmin Is a Critical Regulator of Angiotensin II-Mediated Vascular Remodeling

Y. Hou, K. Okada, C. Okamoto, S. Ueshima and O. Matsuo
Arterioscler Thromb Vasc Biol, July 1, 2008; 28 (7): 1257-1262.
[\[Abstract\]](#) [\[Full Text\]](#) [\[PDF\]](#)

Mitochondrial DNA damage triggers mitochondrial-superoxide generation and apoptosis

C. Ricci, V. Pastukh, J. Leonard, J. Turrens, G. Wilson, D. Schaffer and S. W. Schaffer
Am J Physiol Cell Physiol, February 1, 2008; 294 (2): C413-C422.
[\[Abstract\]](#) [\[Full Text\]](#) [\[PDF\]](#)

Nitric Oxide and Peroxynitrite in Health and Disease

P. Pacher, J. S. Beckman and L. Liaudet
Physiol Rev, January 1, 2007; 87 (1): 315-424.
[\[Abstract\]](#) [\[Full Text\]](#) [\[PDF\]](#)

An integrated view of oxidative stress in aging: basic mechanisms, functional effects, and pathological considerations

K. C. Kregel and H. J. Zhang
Am J Physiol Regulatory Integrative Comp Physiol, January 1, 2007; 292 (1): R18-R36.
[\[Abstract\]](#) [\[Full Text\]](#) [\[PDF\]](#)

Poly(ADP-ribose) polymerase-1-deficient mice are protected from angiotensin II-induced cardiac hypertrophy

J. B. Pillai, M. Gupta, S. B. Rajamohan, R. Lang, J. Raman and M. P. Gupta
Am J Physiol Heart Circ Physiol, October 1, 2006; 291 (4): H1545-H1553.
[\[Abstract\]](#) [\[Full Text\]](#) [\[PDF\]](#)

Updated information and services including high-resolution figures, can be found at:

<http://ajpheart.physiology.org/cgi/content/full/285/6/H2364>

Additional material and information about *AJP - Heart and Circulatory Physiology* can be found at:

<http://www.the-aps.org/publications/ajpheart>

This information is current as of November 11, 2009 .

Apoptotic cascade initiated by angiotensin II in neonatal cardiomyocytes: role of DNA damage

Valentina Grishko,¹ Viktor Pastukh,¹ Viktoriya Solodushko,¹
Mark Gillespie,¹ Junichi Azuma,² and Stephen Schaffer¹

¹Department of Pharmacology, University of South Alabama College of Medicine, Mobile, Alabama 36688; and

²Department of Clinical Evaluation of Medicine and Therapeutics, Osaka University, Osaka 565-0871, Japan

Submitted 15 May 2003; accepted in final form 17 July 2003

Grishko, Valentina, Viktor Pastukh, Viktoriya Solodushko, Mark Gillespie, Junichi Azuma, and Stephen Schaffer. Apoptotic cascade initiated by angiotensin II in neonatal cardiomyocytes: role of DNA damage. *Am J Physiol Heart Circ Physiol* 285: H2364–H2372, 2003. First published August 14, 2003; 10.1152/ajpheart.00408.2003.—Angiotensin II contributes to ventricular remodeling by promoting both cardiac hypertrophy and apoptosis; however, the mechanism underlying the latter phenomenon is poorly understood. One possibility that has been advanced is that angiotensin II activates NADPH oxidase, generating free radicals that trigger apoptosis. In apparent support of this notion, it was found that angiotensin II-mediated apoptosis in the cardiomyocyte is blocked by the NADPH oxidase inhibitor diphenylene iodonium. However, three lines of evidence suggest that peroxynitrite, rather than superoxide, is responsible for angiotensin II-mediated DNA damage and apoptosis. First, the inducible nitric oxide inhibitor aminoguanidine prevents angiotensin II-induced DNA damage and apoptosis. Second, based on ligation-mediated PCR, the pattern of angiotensin II-induced DNA damage resembles peroxynitrite-mediated damage rather than damage caused by either superoxide or nitric oxide. Third, angiotensin II activates p53 through the phosphorylation of Ser15 and Ser20, residues that are commonly phosphorylated in response to DNA damage. It is proposed that angiotensin II promotes the oxidation of DNA, which in turn activates p53 to mediate apoptosis.

NADPH oxidase; peroxynitrite; p53; Bax; Bcl-2; mitochondrial DNA; inducible nitric oxide synthase

ANGIOTENSIN II (ANG II) initiates a wide range of actions through its type 1 (AT₁) and type 2 (AT₂) receptors. Whereas the AT₁ receptor regulates fluid balance, hormone secretion, blood pressure, and myocyte hypertrophy (9, 14, 24), the AT₂ receptor has been implicated in cell growth, proliferation, and differentiation (4, 41). Both receptors appear to trigger cascades that lead to apoptosis. It has been proposed that AT₁ receptor-mediated apoptosis may occur secondary to vascular growth and remodeling, whereas AT₂ receptor-mediated apoptosis opposes cell proliferation. However, the mechanisms underlying these death cascades are poorly defined.

One of the putative AT₂-linked death cascades requires the inactivation of ERK MAPK by a tyrosine phosphatase (35, 42). The observed decrease in ERK activity is thought to reduce the phosphorylation state and activity of the antiapoptotic factor Bcl-2. In PC12W cells, the inhibition of nerve growth factor-mediated Bcl-2 phosphorylation by ANG II leads to the induction of apoptosis (15). However, in the same cell line, a tyrosine phosphatase also promotes ceramide synthesis, an event that is linked to apoptosis (20). A tyrosine phosphatase has also been shown to regulate the phosphatidylinositol 3-kinase/Akt survival pathway (5).

Another AT₂-mediated death cascade proceeds through p38 MAPK. Miura and Karnik (28) have reported that, whereas AT₂-mediated reductions in ERK activity do not alter the number of A7r5 cells that undergo apoptosis, the inhibition of p38 MAPK reduces apoptosis caused by the overstimulation of the AT₂ receptor. A role for the proapoptotic factor Bax in ANG II-mediated apoptosis also deserves consideration because the AT₂ receptor has been reported to upregulate Bax (15).

In both glomerular visceral epithelial cells and rat blood vessels, ANG II-mediated apoptosis involves both AT₁ and AT₂ receptors (6, 7). Although the mechanism by which both receptors contribute to apoptosis has not been established, ANG II-mediated apoptosis in the epithelial cell appears to involve the upregulation of Bax by both AT₁ and AT₂ receptors and a reduction in Bcl-2 content by the AT₁ receptor (7). In contrast, AT₁-mediated elevations in Bax appear to be more important in blood vessel apoptosis (6).

In the cardiomyocyte, the upregulation of Bax appears to be solely AT₁ mediated (33). In 1998, Leri et al. (21) found that stretched myocytes undergo apoptosis in an AT₁-dependent manner. Cell stretching was found to increase p53 and Bax content, leading to the suggestion that ANG II might activate p53, which in turn would upregulate Bax. However, in a subsequent study, Leri et al. (22) found that the activation of p53 was upstream from ANG II generation in the stretched myocyte. Therefore, it was

Address for reprint requests and other correspondence: S. Schaffer, Univ. of South Alabama School of Medicine, Dept. of Pharmacology, Mobile, AL 36688 (E-mail: sschaffe@jaguar1.usouthal.edu).

The costs of publication of this article were defrayed in part by the payment of page charges. The article must therefore be hereby marked "advertisement" in accordance with 18 U.S.C. Section 1734 solely to indicate this fact.

suggested that ANG II might promote apoptosis by activating Ca^{2+} -dependent DNase I, an effect dependent on the activation of PKC and an elevation in intracellular Ca^{2+} concentration (18, 22). AT_1 -mediated apoptosis in human coronary artery endothelial cells and lung alveolar epithelial cells also appears to require the activation of PKC (23, 29).

Therefore, some key steps in the signaling pathways for both AT_1 - and AT_2 -mediated apoptosis have been identified; however, the actual sequence of events leading to programmed cell death is poorly defined. The present study introduces a logical cascade for AT_1 -mediated apoptosis in the isolated rat cardiomyocyte. The proposed cascade takes into consideration the potential role of PKC in both the stimulation of NADPH oxidase and induction of apoptosis (18, 23, 29, 40). Moreover, the hypothesis recognizes the central role of NADPH oxidase and free radical-mediated DNA damage in initiating apoptosis.

EXPERIMENTAL PROCEDURES

Cardiomyocyte preparation and incubation conditions. All care and treatment of animals were in accordance with the guidelines of the National Institute of Health and subjected to prior approval by the Institutional Care and Use Committee of the University of South Alabama. Rat neonatal cardiomyocytes were prepared as described previously (37, 38). The cells were suspended in minimal essential medium containing 10% newborn calf serum and 0.1 mM 5'-bromo-2'-deoxyuridine and allowed to plate on either glass coverslips or polystyrene-treated petri dishes (430167, Corning) at a density of $\sim 10 \times 10^6$ cells/dish (10 cm diameter). They were then placed in serum-free medium containing minimal essential medium for a period of 3 days. The cells were then exposed to medium supplemented with either no addition (control), 10 μM diphenylene iodonium (DPI), 1 nM ANG II, 1 nM ANG II + 10 μM DPI, 0.5 mM aminoguanidine (AG), or 0.5 mM aminoguanidine + 1 nM ANG II. The concentrations of ANG II, DPI, and AG were chosen based on their abilities to induce apoptosis (18), inhibit NADPH oxidase (40), and selectively inhibit inducible nitric oxide (NO) synthase (iNOS) (26). At the appropriate time, the cells were either used for analysis of apoptosis, Western blot analysis, or Southern blot analysis.

Annexin V and propidium iodide procedures. To assess the number of apoptotic and dead cells, the TACS Annexin V-FITC kit was used. After 6 h of exposure to control medium or medium supplemented with ANG II, AG, DPI, or a combination of these factors, the culture medium was removed from the cells. The cells were first rinsed with cold $1 \times$ PBS buffer and then placed in 100 μl of annexin V incubation reagent consisting of 10 μl of $10 \times$ binding buffer, 10 μl of propidium iodide, 1 μl of annexin V conjugate, and 79 μl of distilled water. After a 15-min incubation in the dark with the annexin V reagent, the cells were washed for 2 min with an excess of $1 \times$ binding buffer [100 mM HEPES (pH 7.4), 1.5 M NaCl, 50 mM KCl, 10 mM MgCl_2 , and 18 mM CaCl_2]. Annexin V and propidium iodide staining were observed by fluorescence microscopy using an Olympus IX 70 inverted microscope.

Western blot analyses. Cellular content of Bax, Bcl-2, p53, p53 (phosphorylated Ser¹⁵), p53 (phosphorylated Ser²⁰), and caspase 9 were determined by Western blot analysis using a modification of methods described previously (37, 38). To dislodge the cells from the bottom of the petri dishes, the cells were incubated for 5–7 min with medium containing trypsin. They

were then centrifuged at 500 g for 5 min. After the cells were washed with PBS, they were suspended in lysis buffer [62.5 mM Tris (pH 6.8) containing 2% (wt/vol) SDS and 10% glycerol, to which was added 1 mM orthovanadate, 0.1 mg PMSF, and a 1/100 dilution of protease inhibitor cocktail (Calbiochem)]. The cells were disrupted by drawing them into a pipette and then discharging them several times. The samples were then heated to 95–100°C for 5 min and placed on ice for 15 min. The samples were subjected to SDS-PAGE (12% for Bcl-2, Bax, and caspase 9; 8% for p53 and the phosphorylated forms of p53). The proteins were then transferred to nitrocellulose membranes, where they were blocked. After incubation with the appropriate antibody (purchased from Santa Cruz and Cell Signaling), the membranes were washed and then incubated with a secondary antibody, goat anti-rabbit IgG. The Western blots were detected by the enhanced chemiluminescence reaction. All data were analyzed by densitometry using ChemiImage 4400 (Alpha Innotech).

Detection of mitochondrial DNA damage using quantitative Southern blots. Isolated neonatal cardiomyocytes were exposed to 1 nM ANG for various periods of time. In some experiments, 1 nM ANG was added to the cells in combination with 10 μM DPI or 0.5 mM AG. After the cells were lysed, high-molecular-weight DNA was phenol extracted, precipitated with ammonium acetate, and then exposed to 2 volumes of cold ethanol. The DNA samples were resuspended in water and then digested with the restriction endonuclease *Bam*HIII (10 U/ μg DNA) at the same time it was treated with DNase-free RNase (~ 1.0 /ml) for 12–16 h at 37°C. After digestion, the samples were precipitated with ammonium acetate and resuspended in Tris-EDTA (TE) buffer (10 mM Tris and 1 mM EDTA; pH 8.0). The DNA was precisely quantified using a Hoefer TKO 100 Mini-Fluorometer and a TKO standards kit (Hoefer Scientific Instruments; San Francisco, CA). Samples containing 5 μg DNA were heated at 65°C for 20 min and then cooled at room temperature for an additional 20 min. After NaOH was added to a final concentration of 0.1 N, samples were incubated for 15 min at 37°C. This produced single-strand breaks at any abasic or sugar-modified site in the DNA. Next, samples were combined with 5 μl of loading dye, loaded onto a 0.6% alkaline agarose gel, and electrophoresed at 30 V (1.5 V/cm gel length) for ~ 16 h in an alkaline buffer consisting of 23 mM NaOH and 1 mM EDTA. The gels were stained with ethidium bromide to confirm equal loading. After the gels were washed, DNA was transferred to a Zeta-Probe GT nylon membrane (Bio-Rad; Hercules, CA). The membranes were cross-linked and hybridized with a ³²P-labeled rat mitochondrial DNA-specific PCR-generated probe. Hybridization and subsequent washes were performed according to the manufacturer's recommendations. DNA damage was assessed as follows: break frequency = $-\ln(\text{band intensity after ANG II})/(\text{band intensity of control})$.

Assay for detecting mitochondrial DNA damage at the nucleotide level by ligation-mediated PCR. After treatment, extraction, digestion, and quantitation, 5- to 10- μg aliquots of the DNA samples were heated at 70°C for 20 min and, after being cooled, incubated with 0.1 N NaOH for 15 min. After alkali treatment, DNA samples were precipitated with 0.1 volume of 3 M sodium acetate (pH 5.2) and cold ethanol and then were dissolved in TE buffer. Untreated and alkali-treated DNA (1 μg) from each sample were subjected to ligation-mediated PCR (LM-PCR). Primer extension and ligation were all performed according to Pfeifer et al. (30, 31) with modifications (13). After ligation, the reaction products were precipitated with 0.1 volume of 3 M sodium acetate (pH 5.2), 6.6 mM EDTA (pH 8.0), and 20 μg glycogen and then resuspended in 50 μl H₂O. PCR amplification was performed as previously described (30, 31); the exception being the use of 5 pmol/ μl primer and a longer

oligonucleotide in the asymmetric linker. The increase in the amount of primer used in the LM-PCR was designed to compensate for the increased number of mitochondrial DNA templates present in cells compared with single-copy nuclear genes. After PCR, all samples were precipitated by adding a 25- μ l mixture containing 60 mM EDTA (pH 8.0), 1.6 M sodium acetate (pH 5.2), and 2 volumes of cold ethanol. Pellets were air dried and resuspended in a formamide dye solution containing 57% deionized formamide, 7 mM EDTA, 0.7 mg/ml xylene cyanol FF, and 0.7 mg/ml bromphenol blue. Samples were electrophoresed using regular sequencing gels, blotted, and UV cross-linked to the membrane as previously described (13). Hybridization was performed with a single-strand PCR-generated probe using primer for the appropriate strand. After exposure of the membrane to Kodak XAR, the film density of individual hybridization bands corresponding to nucleotide bases of interest was evaluated by scanning of the radioautographs.

Statistical analysis. The statistical significance of the data was determined using Student's *t*-test for comparison with groups and ANOVA combined with Tukey's post hoc test for comparison between groups. Values of $P < 0.05$ were considered statistically significant.

RESULTS

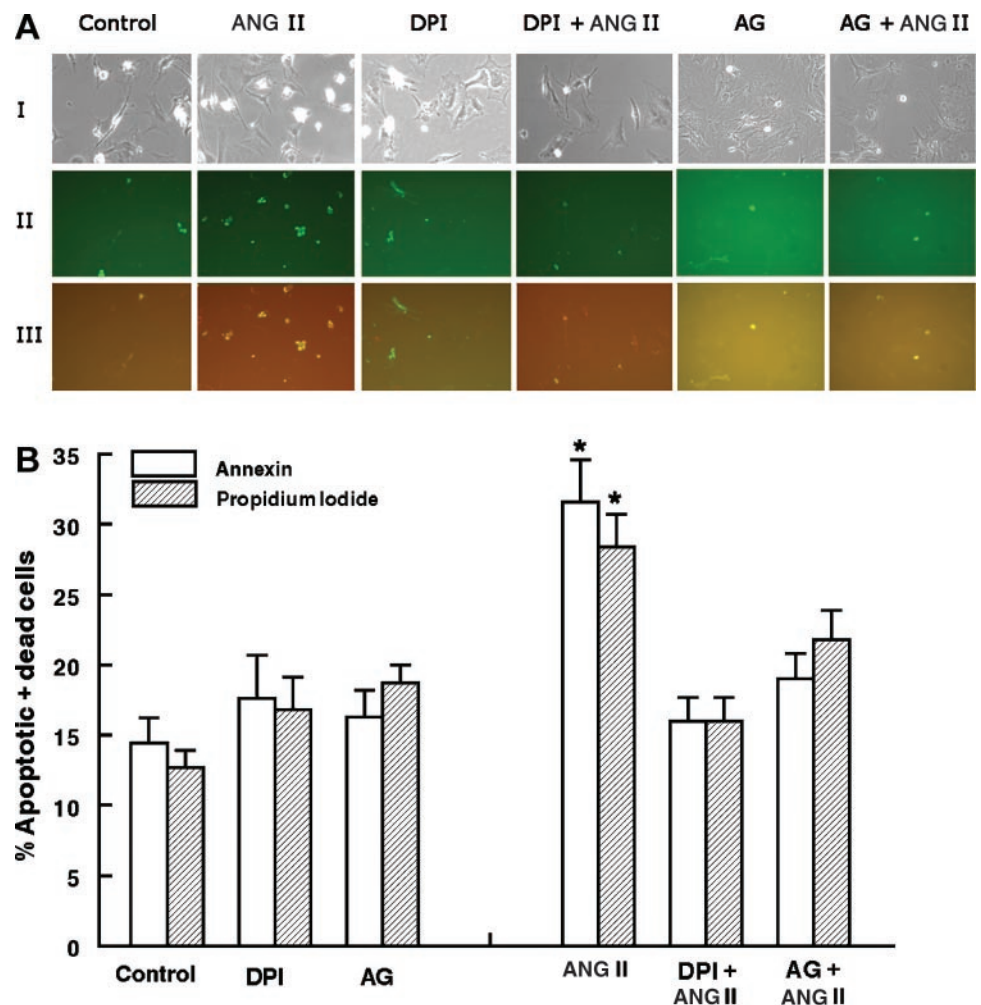
Griendling and Ushio-Fukai (12) proposed that the activation of NADPH oxidase is a key step in ANG II-mediated apoptosis. To examine this hypothesis, iso-

lated neonatal cardiomyocytes were incubated for 6 h with medium containing ANG II and the NADPH oxidase inhibitor DPI. As shown in Fig. 1, ~13% of control cardiomyocytes incubated with medium lacking ANG II and DPI exhibited positive staining for the apoptotic marker annexin V and for the cell death marker propidium iodide. The addition of 10 μ M DPI to the incubation medium lacking ANG II had no significant influence on the number of apoptotic, dead cells (~17%). However, the NADPH oxidase inhibitor completely prevented ANG II-induced apoptosis. Whereas the number of annexin V-positive cells found after 6 h of ANG II treatment was $31.6 \pm 3.0\%$, the number was reduced to $16.0 \pm 1.7\%$ when both 1 nM ANG II and 10 μ M DPI were included in the incubation medium.

Inhibition of NADPH oxidase with DPI also blocked the ANG II-mediated activation of caspase 9 (Fig. 2). In the absence of DPI, ANG II increased the caspase 9-to-procaspase 9 ratio over 70%. However, no significant elevation in the ratio was observed when cells were exposed to both 1 nM ANG II and 10 μ M DPI.

Caspase 9 is an initiator caspase that is activated by the aptosome, a complex formed when cytochrome *c* is released from the mitochondria. One of the major regulators of mitochondrial cytochrome *c* release is the

Fig. 1. Effect of diphenylene iodonium (DPI) and aminoguanidine (AG) on ANG II-induced apoptosis. **A:** isolated neonatal cardiomyocytes were incubated for 6 h with medium containing no additions (control), 10 μ M DPI, 0.5 mM AG, 1 nM ANG II, 10 μ M DPI + 1 nM ANG II, or 0.5 mM AG + 1 nM ANG II. After 6 h of incubation, the cells were incubated for 2 h with the annexin V incubation reagent. The number of cells showing positive staining for annexin V (row II) and propidium iodide (row III) was determined by fluorescence microscopy. Individual cells are shown in row I. **B:** percentage of apoptotic (annexin-stained group) and dead (propidium iodide-stained group) cells. Values are means \pm SE of 8 preparations. *Significant difference between the ANG II treatment group and all other groups ($P < 0.05$).



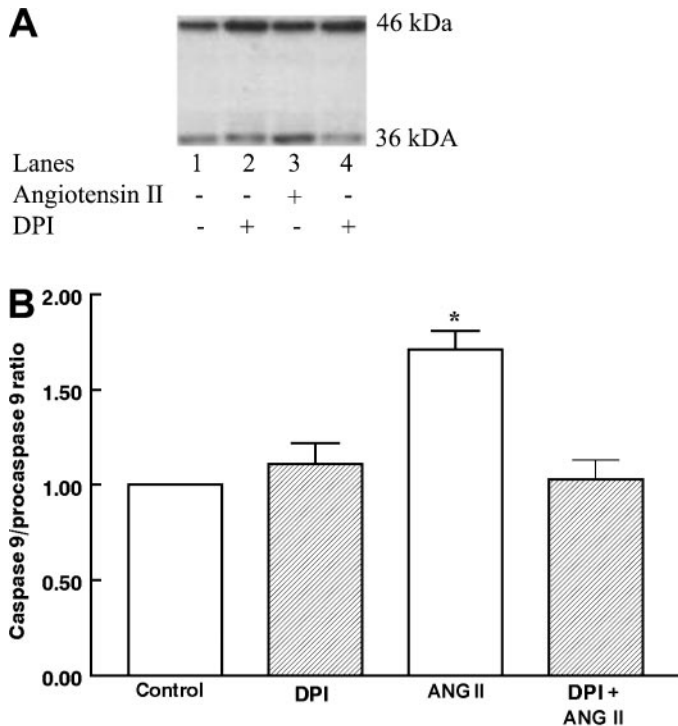


Fig. 2. Role of NADPH oxidase in ANG II-mediated activation of caspase 9. *A*: Western blots for procaspase 9 (46 kDa) and active caspase 9 (36 kDa). Isolated neonatal cardiomyocytes were incubated for 6 h with medium containing either no additions (control), 1 nM ANG II, 10 μ M DPI, or both 1 nM ANG II and 10 μ M DPI. After cell lysis, cellular proteins were separated by 10% SDS-PAGE. The proteins were transferred to nitrocellulose membranes, blocked, and then exposed to an antibody directed against caspase 9. After exposure to goat anti-rabbit IgG, bands were detected by the enhanced chemiluminescence reaction. The levels of caspase 9 and procaspase 9 were determined by densitometry. *B*: ratio of active caspase 9 to procaspase 9. Values are means \pm SE of 4 different preparations. *Significant difference between the ANG II group and the other three groups ($P < 0.05$).

Bcl-2 family of proteins, with Bax promoting the release of cytochrome *c* and Bcl-2 preventing its release (10, 43). Both Bax and Bcl-2 have been previously implicated in ANG II-induced apoptosis (25, 43). Therefore, the effect of DPI on ANG II-induced alterations in the Bax-to-Bcl-2 ratio was examined. In agreement with a previous study (39), it was found that the addition of 1 nM ANG II to the culture medium

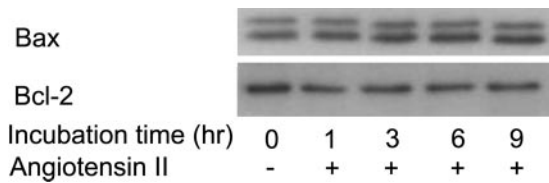


Fig. 3. Effect of ANG II on Bax and Bcl-2 content. Isolated neonatal cardiomyocytes were incubated for various periods of time with medium containing 1 nM ANG II. After cell lysis, cellular proteins were separated by 12% SDS-PAGE. The proteins were transferred to nitrocellulose membranes, blocked, and then exposed to an antibody directed against either Bax or Bcl-2. After exposure to goat anti-rabbit IgG, bands were detected by the enhanced chemiluminescence reaction.

caused a fairly rapid but modest increase in the Bax content of the isolated cardiomyocyte (Fig. 3). ANG II also mediated a modest decrease in the levels of the antiapoptotic factor Bcl-2 (Fig. 3). Treatment of the cells with DPI prevented both the 18% increase in Bax content and the decrease in Bcl-2 content mediated by ANG II (Fig. 4). The net effect of ANG II action was a 40% increase in the Bax-to-Bcl-2 ratio, an action that was completely prevented by the administration of DPI (Fig. 5).

Another regulator of apoptosis that is located upstream of Bax and Bcl-2 is the oncosuppressor gene

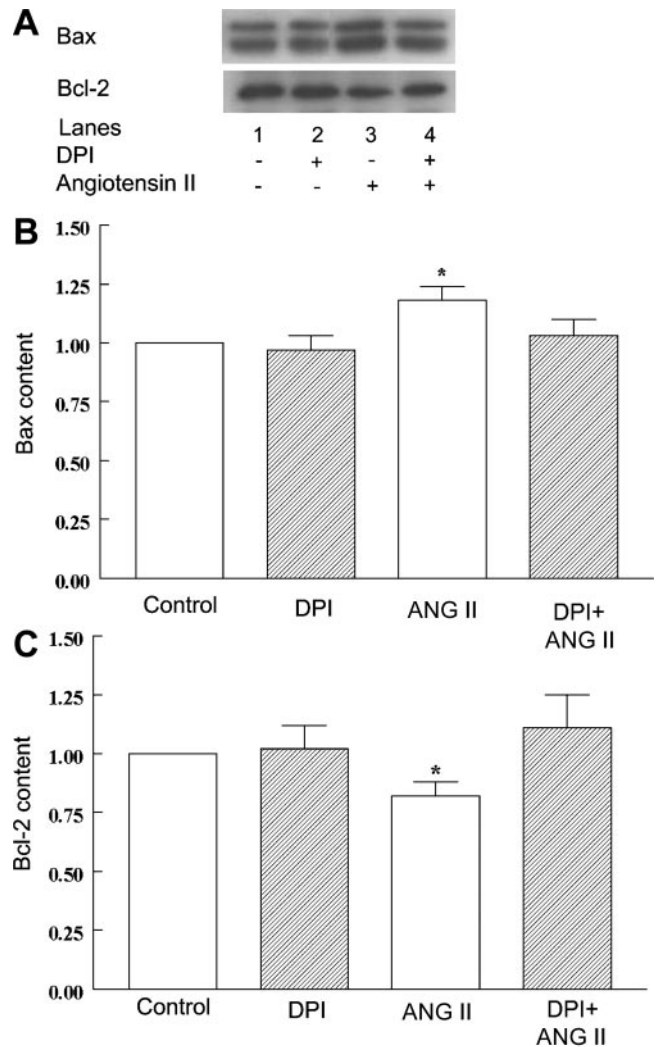


Fig. 4. Role of NADPH oxidase in ANG II-mediated upregulation of Bax and downregulation of Bcl-2. Isolated neonatal cardiomyocytes were incubated for 6 h with medium containing either no additions (control), 1 nM ANG, 10 μ M DPI, or both 1 nM ANG II and 10 μ M DPI. After cell lysis, cellular proteins were separated by 12% SDS-PAGE. The proteins were transferred to nitrocellulose membranes, blocked, and then exposed to an antibody directed against either Bax or Bcl-2. After exposure to goat anti-rabbit IgG, bands were detected by the enhanced chemiluminescence reaction. *B*: levels of Bax were determined by densitometry. *C*: levels of Bcl-2 were determined by densitometry. Values are means \pm SE of 5–7 different preparations. *Significant difference between the ANG II group and the three other groups ($P < 0.05$).

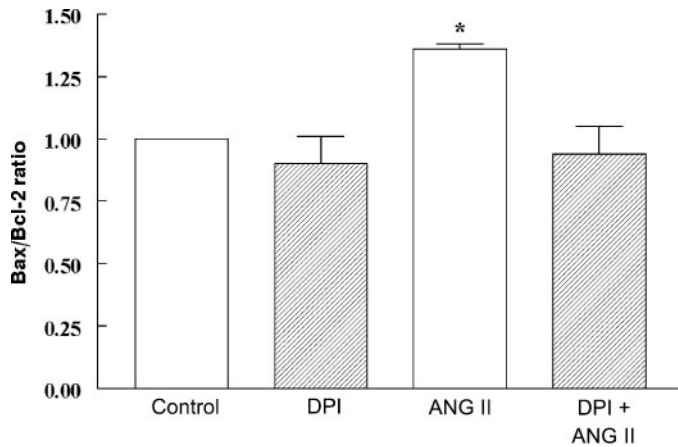


Fig. 5. Effect of ANG II and DPI on the Bax-to-Bcl-2 ratio. The Bax-to-Bcl-2 ratio was calculated from the data shown in Fig. 4.

p53. Several factors regulate the activity of p53 through posttranslational modifications, reduced turnover, and protein induction (19, 36). Two of the post-translational phosphorylation sites of p53 are Ser15 and Ser20. The time course for ANG II-mediated phosphorylation of both Ser15 and Ser20 is shown in Fig. 6. Whereas ANG II-treated cells showed a >50% increase in the amount of phosphorylated Ser15 content after 6 h of ANG II exposure, the elevation in phosphorylated Ser20 content was somewhat less. In contrast, ANG II had no effect on the cellular levels of the total p53 pool (Fig. 6). The addition of DPI to the incubation medium lacking ANG II reduced the levels of phosphorylated Ser20 by 40%, suggesting that the basal rates of NADPH oxidase-mediated superoxide production regulates the phosphorylation state of Ser20. When cells were cotreated with DPI and ANG II, the content of phosphorylated Ser20 was reduced to the level seen in control cells treated with DPI (Fig. 7). Because these levels were 40% below the control, it is clear that NADPH oxidase is involved in the regulation of Ser20 phosphorylation. Although it is likely that NADPH oxidase also regulates the phosphorylation status of Ser15, this could not be ascertained because

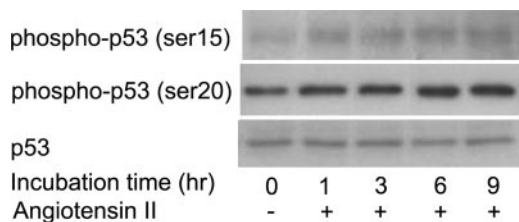


Fig. 6. Effect of ANG II on the phosphorylation status of p53. Western blots for p53 (phosphorylated Ser15), p53 (phosphorylated Ser20), and total p53 are shown. Isolated neonatal cardiomyocytes were incubated for various periods of time with medium containing 1 nM ANG II. After cell lysis, cellular proteins were separated by 10% SDS-PAGE. The proteins were transferred to nitrocellulose membranes, blocked, and then exposed to an antibody directed against p53 or phosphorylated p53, in which either residue Ser15 or Ser20 was phosphorylated. After exposure to goat anti-rabbit IgG, bands were detected by the enhanced chemiluminescence reaction.

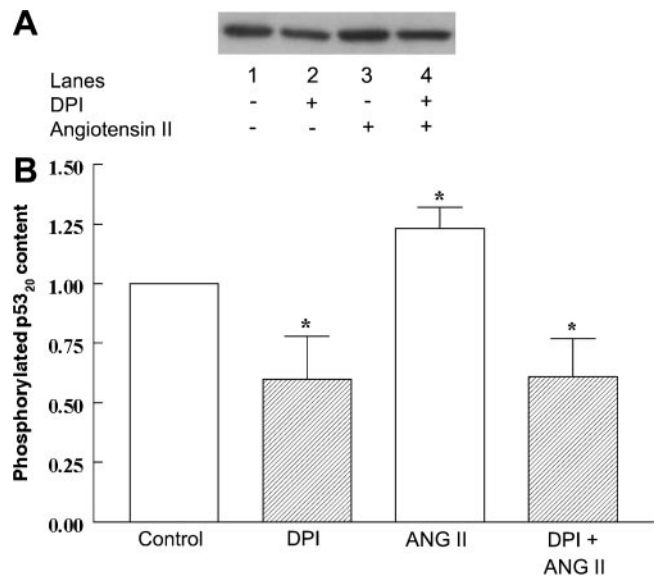


Fig. 7. Effect of NADPH oxidase inhibition on the phosphorylation status of p53 (phosphorylated Ser20). A: isolated neonatal cardiomyocytes were incubated for 6 h with medium containing either no additions (control), 1 nM ANG II, 10 μ M DPI, or both 1 nM ANG II and 10 μ M DPI. After cell lysis, cellular proteins were separated by 10% SDS-PAGE. The proteins were transferred to nitrocellulose membranes, blocked, and then exposed to an antibody directed against p53 (phosphorylated Ser20). After exposure to goat anti-rabbit IgG, bands were detected by the enhanced chemiluminescence reaction. B: levels of p53 (phosphorylated Ser20) were determined by densitometry. Values are means \pm SE of 5–7 different preparations. *Significant difference between the control group and all other groups ($P < 0.05$).

DPI was found to interfere with the Western blot of phosphorylated Ser15 (see Fig. 12).

It is widely accepted that DNA damage activates protein kinases that phosphorylate p53, with two of the favored phosphorylation sites being Ser15 and Ser20. Having already shown that ANG II enhanced the phosphorylation state of p53, we tested the hypothesis that oxidative stress arising from the activation of NADPH oxidase might cause DNA damage. DNA samples from control and ANG II-treated cells were first treated with BamHIII and NaOH and then subjected to Southern blot analysis. As seen in Fig. 8, DNA obtained from ANG II-treated cells exhibited significant reductions in the intensity of the prominent 10-kb band. Because NaOH treatment cleaves DNA at sites of base modifi-

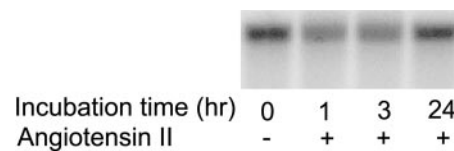


Fig. 8. Mitochondrial DNA damage caused by ANG II. Neonatal cardiomyocytes were incubated for various periods of time with medium containing 1 nM ANG II. High-molecular-weight DNA was isolated and digested to completion with BamHIII. The samples were exposed to 0.1 N NaOH before electrophoresis on a 0.6% agarose gel. After the samples were transferred to nylon membranes, the membranes were hybridized with a 32 P-labeled mitochondrial DNA-specific probe. Bands were visualized by autoradiography.

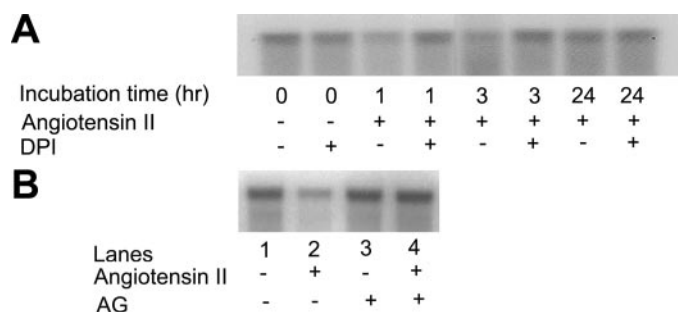


Fig. 9. Role of NADPH oxidase and inducible nitric oxide (NO) synthase (iNOS) in ANG II-mediated mitochondrial DNA damage. *A*: neonatal cardiomyocytes were incubated for various times with medium containing no additions (control), 10 μ M DPI, 1 nM ANG II, or 10 μ M DPI + 1 nM ANG II. High-molecular-weight DNA was isolated and digested to completion with *Bam*HI. The samples were exposed to 0.1 N NaOH before electrophoresis on a 0.6% agarose gel. After the samples were transferred to nylon membranes, the membranes were hybridized with a 32 P-labeled mitochondrial DNA-specific probe. Bands were visualized by autoradiography. *B*: another group of cells was incubated for 1 h with medium containing no additions (control), 0.5 mM AG, 1 nM ANG II, or 0.5 mM AG + 1 nM ANG II. Southern blots were prepared and visualized by autoradiography.

cation, the decreased intensity of the 10-kb band was attributed to both preexisting breaks and NaOH-mediated DNA cleavage. According to the analysis of Grishko et al. (13), the frequency of DNA cleavage after 1 h of ANG II exposure was $\sim 1.0 \pm 0.045$ fragments/10 kb. A similar degree of damage was observed after 3 h of ANG II treatment. However, after 24 h of ANG II exposure, considerably less DNA damage was observed, with the decline likely caused by DNA repair. Figure 9A reveals that treatment of the cells with the NADPH oxidase inhibitor DPI prevented the damage at both 1 and 3 h.

Cai et al. (2) found that hydrogen peroxide derived from NADPH oxidase can promote NO production in bovine aortic endothelial cells. Because NO is also capable of causing DNA damage, the effect of a NOS inhibitor, AG, on ANG II-mediated mitochondrial DNA damage was determined. Interestingly, AG, like DPI, completely blocked ANG II-mediated DNA damage (Fig. 9B).

Grishko et al. (13) have shown that NO modifies DNA by causing the deamination of purines, whereas superoxide-linked ROS cause extensive modification of thymine and guanine. To identify the type of nucleotide damaged, as well as the pattern of ANG II-mediated DNA damage, LM-PCR was performed on a 200-bp stretch of mitochondrial DNA isolated from ANG II-treated cardiomyocytes. This stretch was studied because it contains the common deletion sequence associated with many chronic diseases. For comparison, the pattern of DNA damage mediated by NO (PAPA/NO), superoxide (xanthine oxidase/xanthine), and peroxynitrite was also determined. DNA treated with NaOH contains strands with preexisting breaks and NaOH-induced cleavage sites, whereas DNA treated without NaOH only shows preexisting breaks. On the basis of the Maxim-Gilbert sequencing ladder, most of the

damage caused by NO involved guanine, with adenine also being affected (Figs. 10 and 11). By comparison, peroxynitrite and ANG II preferentially modified guanine and adenine, although some thymine and cytosine residues were also modified. Thymine and guanine served as the favored targets of superoxide. Despite the preferential oxidation of guanine by ANG II and NO, the intensity of damage to specific bases differed between the two agents (Fig. 11). Nonetheless, the pattern of damage was virtually identical for ANG II and peroxynitrite, suggesting that peroxynitrite is the oxidizing agent responsible for ANG II-mediated DNA damage.

Ghafourifar et al. (10) found that stimulation of mitochondrial NOS with calcium is associated with mitochondrial cytochrome *c* release and the induction of apoptosis, a sequence of events prevented by the SOD mimetic manganese (III) tetrakis (4-benzoic acid) porphyrin. Because calcium-induced apoptosis was also prevented by the NOS inhibitor *N*^ω-monomethyl-L-arginine, it was proposed that peroxynitrite might initiate the apoptotic cascade. In a recent review article, Brown and Borutaite (1) proposed that reactive nitrogen species might promote cytochrome *c* release and apoptosis through a p53-linked pathway. Having already confirmed that peroxynitrite was the oxidizing agent responsible for ANG II-mediated DNA damage, we decided to examine the effect of the iNOS inhibitor AG on the phosphorylation status of p53. As shown in

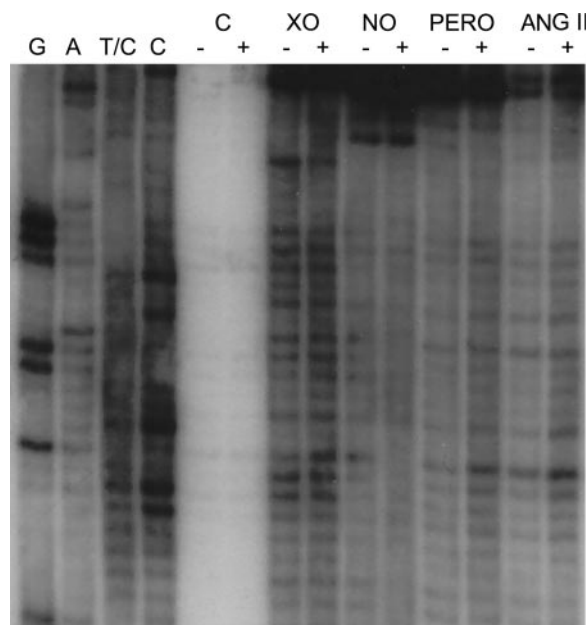


Fig. 10. Effect of various genotoxins on the pattern of mitochondrial DNA damage. Neonatal cardiomyocytes were exposed to medium containing either 50 mU/ml xanthine oxidase plus 0.5 mM hypoxanthine (XO) for 1 h, 50 mM PAPA/NO (NO) for 20 min, 200 μ M peroxynitrite (PERO) for 20 min, or 1 nM ANG II for 3 h. After treatment, cells were lysed and DNA was isolated. The DNA samples were subjected to ligation-mediated PCR. Some of the DNA samples were treated with 0.1 N NaOH (+), whereas others were left untreated (-). NaOH cleaves DNA at the site of base modification. The Maxim-Gilbert ladder defines the location of each base in the DNA sequence.

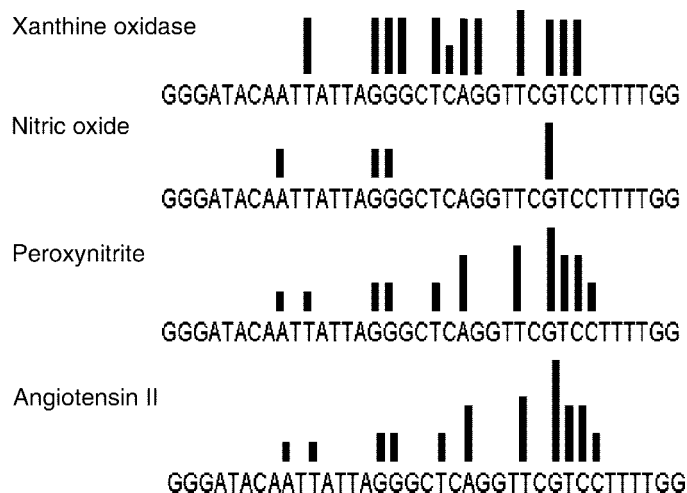


Fig. 11. Nucleotide damage map. The map represents a 37-bp stretch within the 202-bp (position 8172–8208 on the heavy strand of rat mitochondrial DNA) fragment of mitochondrial DNA that was analyzed. The bars located above the specific nucleotides indicate arbitrary values on a scale from 0.5 to 3.5, each value representing the intensity of damage to a particular nucleotide. The damage occurred after exposure of primary neonatal cardiomyocytes to 50 mU/ml xanthine oxidase plus 0.5 mM hypoxanthine (XO), 50 mM PAPA/NO (NO), 200 μ M PERO, or 1 nM ANG II.

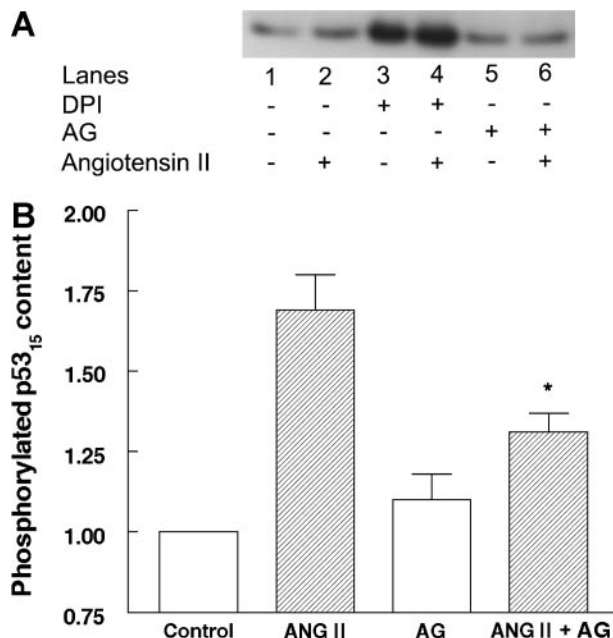


Fig. 12. Effect of DPI and AG on the phosphorylation state of p53 (phosphorylated Ser15). A: isolated neonatal cardiomyocytes were incubated for 6 h with medium containing either no additions (control), 1 nM ANG II, 0.5 AG, 1 nM ANG II + 10 μ M DPI, or 1 nM ANG II + 0.5 mM AG. After cell lysis, cellular proteins were separated by 10% SDS-PAGE. The proteins were transferred to nitrocellulose membranes, blocked, and then exposed to an antibody directed against phosphorylated p53 (Ser15). After exposure to goat anti-rabbit IgG, bands were detected by enhanced chemiluminescence reaction. B: levels of phosphorylated p53 were determined by densitometry. Values are means \pm SE of 4 different preparations. *Significant difference between the ANG II group and the ANG II + AG group ($P < 0.05$).

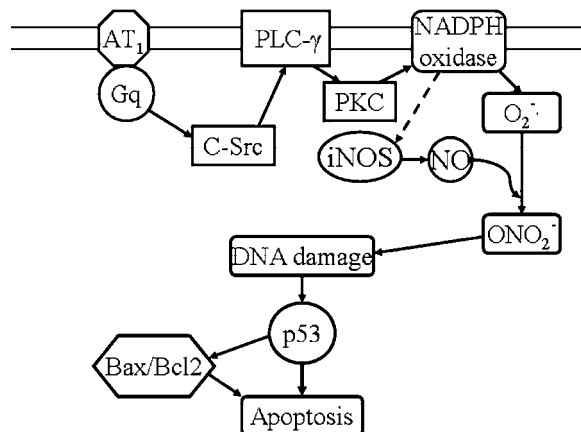


Fig. 13. Scheme of ANG II-mediated apoptosis. AT₁, ANG type 1 receptor; PLC- γ , phospholipase C- γ .

Fig. 12, AG had no major effect on the phosphorylation state of Ser15 in the absence of ANG II. However, the iNOS inhibitor partially prevented the elevation in phosphorylated p53 (Ser15) content seen in the ANG II-treated cell (Fig. 12). Associated with the attenuation in p53 phosphorylation was a reduction in the degree of ANG II-induced apoptosis. Whereas ANG increased the number of annexin V-positive cells from $14.4 \pm 1.8\%$ to $31.6 \pm 3.0\%$, only $19.7 \pm 1.8\%$ of the AG-treated cells became apoptotic after 6 h of ANG II exposure (Fig. 1).

DISCUSSION

Figure 13 shows a proposed scheme for AT₁-mediated apoptosis in the isolated cardiomyocyte. Ishida et al. (17) have shown that one of the earliest detectable events in ANG II signaling is the activation of *c-src*, a tyrosine kinase that stimulates phospholipase C, leading to the formation of diacylglycerol and the activation of PKC. The increase in PKC activity causes an activation of NADPH oxidase, a major source of superoxide (40). ROS generated from NADPH oxidase react with NO to form peroxynitrite (2). On the basis of the pattern of DNA damage, it is proposed that peroxynitrite is the ROS that oxidizes DNA. In response to DNA damage, protein kinases are activated, which in turn phosphorylate and stimulate p53. Apoptosis occurs as a result of p53-mediated elevations in the Bax-to-Bcl-2 ratio and in a p53-dependent mechanism that results in the activation of the mitochondrial death pathway.

It is widely accepted that ANG II activates PKC in the cardiomyocyte (18). Evidence that inhibitors of PKC block ANG II-induced ROS production in vascular smooth muscle cells places PKC upstream from NADPH oxidase (40). In support of this notion, it has been shown that NADPH oxidase can be phosphorylated and activated by PKC in the neutrophil (11). Therefore, the involvement of NADPH oxidase in ANG II-mediated apoptosis is consistent with the view that activation of PKC is a required step in ANG II-induced apoptosis (18).

In 2000, Griendling and Ushio-Fukai (12) proposed that ANG II-mediated ROS could trigger apoptosis.

However, the steps between ROS generation and cell death remained unclear. The present study was designed to clarify some of the steps in this death cascade. One of the initial steps is the formation of peroxynitrite from NO and superoxide. Although the study did not directly examine the effect of ANG II on iNOS activity, it was found that the iNOS inhibitor AG blocked ANG II-induced DNA damage, p53 phosphorylation, and apoptosis. Whether ANG II increased iNOS activity through a signaling pathway that did not involve NADPH oxidase was not determined. Nonetheless, it is significant that Ikeda et al. (16) have shown that ANG II augments interleukin-1 β -mediated NO synthesis, an effect associated with an increase in iNOS mRNA accumulation. Moreover, Cai et al. (2) reported that ANG II-mediated H₂O₂ generation induces endothelial NOS, causing a release of NO. Therefore, it is likely that NADPH oxidase is involved in ANG II-mediated activation of iNOS in the neonatal cardiomyocyte. In other words, NADPH oxidase is responsible for the generation of both factors that combine to form peroxynitrite. Although previous studies have reported on the oxidation of proteins and lipids by peroxynitrite, this is the first report showing that peroxynitrite oxidizes the purine and pyrimidine residues of mitochondrial DNA (Fig. 10). In fact, the pattern of DNA damage by ANG II was virtually identical to that seen with peroxynitrite. As previously reported by Grishko et al. (13), certain guanines are oxidized by PAPA/NO but not by the alkylating agent methylnitrosourea. On the basis of the pattern of DNA damage, it is clear that neither superoxide-derived ROS nor NO directly contribute to ANG II-induced DNA damage. While there are certain similarities between NO-induced DNA damage and ANG II-induced damage, the frequency of individual base damage is most consistent with a role of peroxynitrite in ANG II-induced DNA damage.

The link between DNA damage and p53 activation has been the focus of numerous studies (19, 36). In response to DNA damage, several protein kinases are activated that phosphorylate one or more serine residues of p53. Two of the sites phosphorylated by these protein kinases and by ANG II treatment are Ser15 and Ser20. In addition to promoting the phosphorylation of these regulatory sites on p53, DNA damage also indirectly facilitates the acetylation of lysine residues on the COOH terminus of p53. While the phosphorylation and acetylation reactions also stabilize and reduce the turnover of p53, a p53-linked increase in transcriptional activity can occur in the absence of a large increase in p53 protein content. Indeed, in the present study, ANG II promoted the phosphorylation of p53 but had no significant effect on the protein content of p53. Nonetheless, the increase in the phosphorylation state of Ser15 and Ser20 should cause the DNA binding activity of p53 to rise, resulting in transcriptional activation.

ANG II was found to modestly elevate the levels of Bax in the cardiomyocyte. Although both AT₁ and AT₂ receptors are capable of elevating Bax levels (7), the

elevation of Bax in the cardiomyocyte appears to depend on the cascade initiated by the AT₁ receptor (22, 39). Indeed, the AT₁ receptor blocker losartan, but not the AT₂ receptor blocker PD-123319, is an effective inhibitor of ANG II-mediated apoptosis and the upregulation of Bax in both neonatal and adult cardiomyocytes (3, 18, 22). The elevation in Bax content is most likely caused by p53-dependent transcriptional activation of the proapoptotic factor, an event that is blocked by DPI (25, 43). Nonetheless, an upregulation of Bax is not necessarily a requirement for p53-mediated apoptosis. Regula and Kirshenbaum (34) found that in ventricular myocytes overexpressing wild-type p53, Bax levels were elevated. However, Bax was not elevated in cells that overexpressed a mutant form of p53 defective in gene transcription and that ultimately underwent apoptosis. Moreover, Ding et al. (8) found that p53 participated in radiation-induced apoptosis of myc/ras-transformed rat embryo fibroblasts without the involvement of Bax.

Besides its ability to regulate cellular Bax levels, p53 also downregulates myocardial Bcl-2 levels (32). In the present study, 6 h of ANG II exposure resulted in an 18% decrease in Bcl-2 levels and a 40% increase in the Bax-to-Bcl-2 ratio. Although these changes are modest, the increase in the number of apoptotic cells is also modest. Nonetheless, it is likely that events independent of Bcl-2 family members contribute to ANG II-induced apoptosis. A logical candidate for the initiation of the p53-dependent apoptotic cascade is the impairment in mitochondrial function (27).

DISCLOSURES

This study was supported by National Heart, Lung, and Blood Institute Grant HL-63723.

REFERENCES

1. Brown CG and Borutaite V. Nitric oxide, mitochondria and cell death. *IUBMB Life* 52: 189–195, 2001.
2. Cai H, Li Z, Dikalov S, Hwang J, Jo H, Dudley SC Jr, and Harrison DG. NAD(P)H oxidase-derived hydrogen peroxide mediates endothelial nitric oxide production in response to angiotensin II. *J Biol Chem* 277: 48311–48317, 2002.
3. Cigola E, Kajstura J, Li B, Meggs LG, and Anversa P. Angiotensin II activates programmed myocyte cell death in vitro. *Exp Cell Res* 231: 363–371, 1997.
4. Cook VI, Grove KL, McMenamin KM, Carter MR, Harding JW, and Speth RC. The AT₂ angiotensin receptor subtype predominates in the 18 day gestation fetal rat brain. *Brain Res* 560: 334–336, 1991.
5. Cui TX, Nakagami H, Nahmias C, Shiuchi T, Takeda-Matsumura Y, Li JM, Wu L, Iwai M, and Horiuchi M. Angiotensin II subtype 2 receptor activation inhibits insulin-induced phosphoinositide 3-kinase and Akt and induces apoptosis in PC12W cells. *Mol Endocrinol* 16: 2113–2123, 2002.
6. Diep QN, Li JS, and Schiffrin EL. In vivo study of AT₁ and AT₂ angiotensin receptors in apoptosis in rat blood vessels. *Hypertension* 34: 617–624, 1999.
7. Ding G, Reddy K, Kapasi AA, Frankii N, Gibbons N, Kasinath BS, and Singhal PC. Angiotensin II induces apoptosis in rat glomerular epithelial cells. *Am J Physiol Renal Physiol* 283: F173–F180, 2002.
8. Ding HF, McGill G, Rowan S, Schmaltz C, Shimamura A, and Fisher DE. Oncogene-dependent regulation of caspase activation by p53 protein in a cell-free system. *J Biol Chem* 273: 28378–28383, 1998.

9. **Everett AD, Tufro-McReddie A, Fisher A, and Gomez RA.** Angiotensin receptor regulates cardiac hypertrophy and transforming growth factor-beta 1 expression. *Hypertension* 23: 587–592, 1994.
10. **Ghafourifar P, Schenk U, Klein SD and Richter C.** Mitochondrial nitric-oxide synthase stimulation causes cytochrome c release from isolated mitochondria. *J Biol Chem* 274: 31185–31188, 1999.
11. **Griendling KK, Sorescu D, and Ushio-Fukai M.** NAD(P)H oxidase: role in cardiovascular biology and disease. *Circ Res* 86: 494–501, 2000.
12. **Griendling KK and Ushio-Fukai M.** Reactive oxygen species as mediators of angiotensin II signaling. *Regul Pept* 91: 21–27, 2000.
13. **Grishko VI, Druzhyna N, LeDoux SP, and Wilson GL.** Nitric oxide-induced damage to mtDNA and its subsequent repair. *Nucleic Acids Res* 27: 4510–4516, 1999.
14. **Hogarty DC, Speakman EA, Puig V, and Phillips MI.** The role of angiotensin, AT₁ and AT₂ receptors in the pressor, drinking and vasopressin responses to central angiotensin. *Brain Res* 586: 289–294, 1992.
15. **Horiuchi M, Akishita M, and Dzau VJ.** Recent progress in angiotensin II type 2 receptor research in the cardiovascular system. *Hypertension* 33: 613–621, 1999.
16. **Ikeda U, Maeda Y, Kawahara Y, Yokoyama M, and Shimada K.** Angiotensin II augments cytokine-stimulated nitric oxide synthesis in rat cardiac myocytes. *Circulation* 92: 2683–2689, 1995.
17. **Ishida M, Marrero MB, Schieffer B, Ishida T, Bernstein KE, and Berk BC.** Angiotensin II activates pp60c-src in vascular smooth muscle cells. *Circ Res* 77: 1053–1059, 1995.
18. **Kajstura J, Cigola E, Malhotra A, Li P, Cheng W, Meggs LG, and Anversa P.** Angiotensin II induces apoptosis of adult ventricular myocytes in vitro. *J Mol Cell Cardiol* 29: 859–870, 1997.
19. **Lakin ND and Jackson SP.** Regulation of p53 in response to DNA damage. *Oncogene* 18: 7644–7655, 1999.
20. **Lehtonen JYA, Horiuchi M, Daviet L, Akishita M, and Dzau VJ.** Activation of the de novo biosynthesis of sphingolipids mediates angiotensin II type 2 receptor-induced apoptosis. *J Biol Chem* 274: 16901–16906, 1999.
21. **Leri A, Claudio PP, Li Q, Wang X, Reiss K, Wang S, Malhotra A, Kajstura J, and Anversa P.** Stretch-mediated release of angiotensin II induces myocyte apoptosis by activating p53 that enhances the local renin-angiotensin system and decreases the Bcl-2-to-Bax protein ratio in the cell. *J Clin Invest* 101: 1326–1342, 1998.
22. **Leri A, Fiordaliso F, Setoguchi M, Limana F, Bishopric NH, Kajstura J, Webster K, and Anversa P.** Inhibition of p53 function prevents renin-angiotensin system activation and stretch-mediated myocyte apoptosis. *Am J Pathol* 157: 843–857, 2000.
23. **Li D, Yang B, Philips MI, and Mehta JL.** Proapoptotic effects of ANG II in human coronary artery endothelial cells: role of AT₁ receptor and PKC activation. *Am J Physiol Heart Circ Physiol* 276: H786–H792, 1999.
24. **Lyall F, Dornan ES, McQueen J, Boswell F, and Kelly M.** Angiotensin II increases proto-oncogene expression and phosphoinositide turnover in vascular smooth muscle cells via the angiotensin II AT₁ receptor. *J Hypertens* 10: 1463–1469, 1992.
25. **McCurrach M, Connor TMF, Knudson CM, Korsmeyer SJ, and Lowe SW.** Bax-deficiency promotes drug resistance and oncogenic transformation by attenuating p53-dependent apoptosis. *Proc Natl Acad Sci USA* 94: 2345–2349, 1997.
26. **Misko TP, Moore WM, Kasten TP, Nickols GA, Corbett Tilton RG JA, McDaniel ML, Williamson JR, and Currie MG.** Selective inhibition of the inducible nitric oxide synthase by aminoguanidine. *Eur J Pharmacol* 233: 119–125, 1993.
27. **Moll UM and Zaika A.** Nuclear and mitochondrial apoptotic pathways of p53. *FEBS Lett* 493: 65–69, 2001.
28. **Miura SI and Karnik SS.** Ligand-independent signals from angiotensin II type 2 receptor induce apoptosis. *EMBO J* 19: 4026–4035, 2000.
29. **Papp M, Li X, Zhuang J, Wang R, and Uhal BD.** Angiotensin receptor subtype AT₁ mediates alveolar epithelial cell apoptosis in response to ANG II. *Am J Physiol Lung Cell Mol Physiol* 282: L713–L718, 2002.
30. **Pfeifer GP, Drouin R, and Holmquist GP.** Detection of DNA adducts at the DNA sequence level by ligation-mediated PCR. *Mutat Res* 288: 39–46, 1993.
31. **Pfeifer GP, Drouin R, Riggs AD, and Holmquist GP.** In vivo mapping of a DNA adduct at nucleotide resolution: detection of pyrimidine (6–4)pyrimidone photoproducts by ligation-mediated polymerase chain reaction. *Proc Natl Acad Sci USA* 88: 1374–1378, 1991.
32. **Pierzchalski P, Reiss K, Cheng W, Cirielli C, Kajstura J, Nitahara JA, Rizk M, Capogrossi MC, and Anversa P.** p53 Induces myocyte apoptosis via the activation of the renin-angiotensin system. *Exp Cell Res* 234: 57–65, 1997.
33. **Ravassa S, Fortuno MA, Gonzalez A, Lopez B, Zalba G, and Diez J.** Mechanisms of increased susceptibility to angiotensin II-induced apoptosis in ventricular cardiomyocytes of spontaneously hypertensive rats. *Hypertension* 36: 1065–1071, 2000.
34. **Regula KM and Kirshenbaum LA.** p53 activates the mitochondrial death pathway and apoptosis of ventricular myocytes independent of de novo gene transcription. *J Mol Cell Cardiol* 33: 1435–1445, 2001.
35. **Roessig L, Hermann C, Haendeler J, Zeiher AM, and Dimmeler S.** Angiotensin II-induced upregulation of MAP kinase phosphatase-3 mRNA levels mediates endothelial cell apoptosis. *Basic Res Cardiol* 97: 1–8, 2002.
36. **Sakaguchi K, Herrera JE, Saito S, Miki T, Bustin M, Vassilev A, Anderson CW, and Appella E.** DNA damage activates p53 through a phosphorylation-acetylation cascade. *Genes Dev* 12: 2831–2841, 1998.
37. **Schaffer SW, Ballard Croft C, and Solodushko V.** Cardio-protective effect of chronic hyperglycemia: effect on hypoxia-induced apoptosis and necrosis. *Am J Physiol Heart Circ Physiol* 278: H1948–H1954, 2000.
38. **Schaffer S, Solodushko V, and Kakhniashvili D.** Beneficial effect of taurine depletion on osmotic sodium and calcium loading during chemical hypoxia. *Am J Physiol Cell Physiol* 282: C1113–C1120, 2002.
39. **Schaffer S, Solodushko V, Pastukh V, Ricci C, and Azuma J.** Possible cause of taurine deficient cardiomyopathy: potentiation of angiotensin II action. *J Cardiovasc Pharmacol* 41: 751–759, 2003.
40. **Seshiah PN, Weber DS, Rocic P, Valppu L, Taniyama Y, and Griendling KK.** Angiotensin II stimulation of NAD(P)H oxidase activity: upstream mediators. *Circ Res* 91: 406–413, 2002.
41. **Stoll M, Steckelings UM, Paul M, Bottari SP, Metzger R, and Unger T.** The angiotensin AT₂-receptor mediates inhibition of cell proliferation in coronary endothelial cells. *J Clin Invest* 95: 651–657, 1995.
42. **Xiang H, Kinoshita Y, Knudson CM, Korsmeyer SJ, Schwartzkroin PA, and Morrison RS.** Bax involvement in p53-mediated neuronal cell death. *J Neurosci* 18: 1363–1373, 1998.
43. **Yamada T, Horiuchi M, and Dzau VJ.** Angiotensin II type 2 receptor mediates programmed cell death. *Proc Natl Acad Sci USA* 93: 156–160, 1996.